# Properties and Reactivity of Myoglobin Reconstituted with Chemically Modified Protohemin Complexes†

Enrico Monzani,‡ Gloria Alzuet,‡,§ Luigi Casella,*,‡ Cristina Redaelli,‡ Cristina Bassani,‡ Anna Maria Sanangelantoni,|| Michele Gullotti,⊥ Luca De Gioia,⊥ Laura Santagostini,⊥ and Francesco Chillemi#

*Dipartimento di Chimica Generale, Università di Pavia, Via Taramelli 12, 27100 Pavia, Italy, Dipartimento di Genetica e Microbiologia, Università di Pavia, 27100 Pavia, Italy, Dipartimento di Chimica Inorganica, Metallorganica e Analitica, Università di Milano, Centro CNR, Via Venezian 21, 20133 Milano, Italy, Dipartimento di Chimica Organica e Industriale, Università di Milano, Via Venezian 21, 20133 Milano, Italy*

*Received April 6, 2000; Revised Manuscript Received May 23, 2000*

ABSTRACT: The synthetic complexes protohemin-6(7)-L-arginyl-L-alanine (HM-RA) and protohemin-6(7)-L-histidine methyl ester (HM-H) were prepared by condensation of suitably protected Arg-Ala or His residues with protohemin IX. HM-RA and HM-H were used for reconstitution of apomyoglobin from horse heart, yielding the Mb-RA and Mb-H derivatives, respectively, of the protein. The spectral, binding and catalytic properties of Mb-RA and Mb-H are significantly different from those of Mb. As shown by MM and MD calculations, these differences are determined by some local structural changes around the heme which are generated by increased mobility of a key peptide segment (Phe43−Lys47), containing the residue (Lys45) that in native Mb interacts with one of the porphyrin carboxylate groups. In the reconstituted Mbs this carboxylate group is bound to the Arg−Ala or His residue and is no longer available for electrostatic interaction with Lys45. The mobility of the peptide segment near the active site allows the distal histidine to come to a closer contact with the heme, and in fact Mb-RA and Mb-H exist as an equilibrium between a high-spin form and a major low-spin, six-coordinated form containing a bis-imidazole ligated heme. The two forms are clearly distinguishable in the NMR spectra, that also show that each of them consists of a mixture of the two most stable isomers resulting from cofactor reconstitution, as also anticipated by MM and MD calculations. Exogenous ligands such as cyanide, azide, or hydrogen peroxide can displace the bound distal histidine, but their affinity is reduced. On the other hand, mobilization of the peptide chain around the heme in the reconstituted Mbs increases the accessibility of large donor molecules at the heme periphery, with respect to native Mb, where a rigid backbone limits access to the distal pocket. The increased active site accessibility of Mb-RA and Mb-H facilitates the binding and electron transfer of phenolic substrates in peroxidase-type oxidations catalyzed by the reconstituted proteins in the presence of hydrogen peroxide.

The understanding of the mechanisms by which protein structure controls the catalytic activity of heme proteins is of considerable current interest (*1*−*4*). Myoglobin (Mb)[1] is extensively studied as a model to explore the role of amino acid residues in the distal pocket (*5*−*10*) and of the proximal axial ligand (His93) (*11*−*15*) by site directed mutagenesis. An important goal of these experiments is the introduction of useful catalytic activities into a readily available protein (*9*−*12*), to mimic the oxidative processes exhibited, for instance, by cytochromes P-450, peroxidases, and catalases. In the present work we explore an alternative approach to genetic engineering to obtain Mb derivatives with catalytic properties. This is based on the reconstitution of apomyoglobin with suitably modified, synthetic heme prosthetic groups. Reconstitution of apomyoglobin has been widely studied in the past (*16*−*20*), but the main scope of the latter investigations was to gain an understanding of the interactions that stabilize heme binding to the globins. Only recently a report on enhanced peroxidase activity by Mb reconstituted with a heme group bearing eight carboxylates bound to the

† This work was supported by the Italian MURST.

* To whom correspondence should be addressed. Phone:+39-0382-507331. Fax: +39-0382-528544. E-mail: bioinorg@unipv.it.

‡ Dipartimento di Chimica Generale.

§ Present address: Departamento de Quimica Inorganica, Facultad de Farmacia, Avda. Vicent Andres Estelles. 46100-Burjassot (Valencia), Spain.

|| Dipartimento di Genetica e Microbiologia.

⊥ Dipartimento di Chimica Inorganica.

# Dipartimento di Chimica Organica e Industriale.

[1] Abbreviations: DMF, dimethylformamide; Fmoc, 9-fluorenylmethoxycarbonyl; HOBt, 1-hydroxybenzotriazole; Pmc, 2,2,5,7,8-pentamethylchroman-6-sulphonyl; Z, benzyloxycarbonyl; DCC, dicyclohexylcarbodiimide; OPfp, pentafluorophenoxy; HBTU, *O*-benzotriazol-1-yl-*N*,*N*,*N*′,*N*′-tetramethyluronium hexafluorophosphate; ABTS, 2,2′-azino-bis(3-ethylbenz-thiazoline-6-sulfonic acid; Mb, myoglobin; HM, protohemin IX; HM-RA, protohemin-6(7)-L-arginyl-L-alanine; Mb-RA, myoglobin reconstituted with HM-RA; HM-H, protohemin-6(7)-L-histidine methyl ester; Mb-H, myoglobin reconstituted with HM-H; Mb-HA, hypothetical myoglobin reconstituted with protohemin-6(7)-L-histidyl-L-alanine; HRP, horseradish peroxidase; RZ, Reinheitszahl (purity index, $A_{Soret}/A_{280}$); CD, circular dichroism; NMR, nuclear magnetic resonance; TLC, thin-layer chromatography; FABMS, fast atom bombardment mass spectrometry; MM, molecular mechanics; MD, molecular dynamics.

10.1021/bi000784t CCC: $19.00 
Published on Web 07/08/2000

Scheme 1

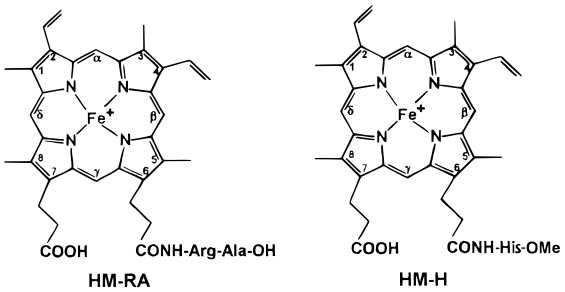


propionate side chains has appeared (*21*). The approach followed here stems from our previous studies on the synthesis and catalytic activity of heme-peptide complexes (*22*−*24*), where peptide residues of variable length were covalently attached to the propionic acid side chains of deuterohemin.

A key role in the catalytic mechanism of peroxidases is apparently played by the invariant histidine and arginine distal residues (*3*, *25*). These facilitate peroxide binding and cleavage at the iron site and may also stabilize the compound I intermediate, as shown, for instance, by the finding that replacement of distal histidine or distal arginine with leucine residues in cytochrome *c* peroxidase gives mutants with strongly reduced rates of compound I formation (*26*). Similar conclusions were drawn by engineering of the distal residues of other peroxidases (*27*−*31*). We thus thought that by reconstitution of apomyoglobin with a hemin modified by covalent attachment of an arginine residue it might be possible to obtain a protein with enhanced peroxidase activity. To this end we have synthesized the hemin complex HM-RA (Scheme 1) and replaced with this the original Mb prosthetic group, yielding the reconstituted Mb-RA derivative. We also synthesized the related hemin derivative HM-H, containing a covalently attached histidine residue, and studied, in parallel, the properties of the two reconstituted Mbs. Since the function of distal arginine in peroxidases is essentially connected with its positive charge, a similar role may be played by an imidazole group, which is partially protonated at physiological pH. The reconstituted Mb-H protein proved important to gain an understanding of the reconstituted Mbs in terms of cofactor reconstitution mode.

## EXPERIMENTAL PROCEDURES

Horse heart myoglobin and horseradish peroxidase (Type VI, RZ = 3.2 at pH 7.0) and protohemin chloride were commercially available (Sigma). The synthesis of the hemin complex HM-H was performed following the same procedure used to prepare the corresponding deuterohemin complex (*23*) and is reported elsewhere (*32*). The other chemicals were reagent grade and used as received. Dimethylformamide was purified by treatment with barium oxide and distilled from calcium hydride under reduced pressure before use. Buffers were prepared using deionized, double distilled water. Hydrogen peroxide solutions were prepared by dilution of a 30% (v/v) solution and the exact concentration was determined by iodimetric titration before use. Optical absorbance spectra and conventional kinetic experiments were studied with an HP-8452A diode array spectrophotometer. Fast kinetic experiments were performed with a Model RS-1000 Applied Photophysics thermostated stopped-flow apparatus, with dead time of 1 ms and 1-cm path length. FABMS spectra were obtained with a VG 7070 EQ spectrometer. CD spectra were recorded on a Jasco J-710 dichrograph calibrated with a solution of isoandrosteron in dioxane ($\Delta\epsilon$ = +3.31 $M^{-1}$ $cm^{-1}$ at 304 nm). Determination of secondary structure contributions was carried out by fitting of the CD spectra (190−240 nm) according to a program available from Jasco. Proton NMR spectra were obtained with a Bruker Avance spectrometer operating at 400 MHz. TLC analysis of the synthetic peptides was performed on Merck Kieselgel 60 plates in the solvent system: benzene, ethyl acetate, acetic acid, and water (10:10:2:1, v/v/v/v); the aqueous phase was discarded.

*Preparation of Fmoc-Arg(Pmc)-Ala-O-tBu*. Fmoc-Arg-(Pmc)-OH (3.31 g, 5 mmol), H-Ala-O-*t*Bu (1.5 g, 5 mmol) and HOBt (0.76 g, 5 mmol) were dissolved in DMF (75 mL). To the ice cold solution was added DCC (1.1 g, 5 mmol), and the mixture was allowed to react with stirring for 2 h at 0 °C and overnight at room temperature. The reaction mixture was filtered, and the filtrate was evaporated to dryness under vacuum. The residue was dissolved in ethyl acetate and washed with HCl 0.1 M at 0 °C, water, saturated $NaHCO_3$, and water. The organic phase was dried ($Na_2SO_4$) and evaporated to dryness in a vacuum. The crude material was recrystallized from ethanol, diethyl ether, and petroleum ether. Yield 3.29 g (81%). mp 144−146 °C; $R_f$ = 0.85; $[\alpha]_D$ = −11.1° (c 1, ethanol). Anal. Calcd. for $C_{42}H_{55}N_5O_8S$: C, 63.85; H, 7.02; N, 8.86. Found: C, 63.67; H, 7.11; N, 8.79.

*Preparation of Protohemin-6(7)-L-arginyl-*L*-alanine (HM-RA)*. Removal of the Fmoc protecting group at the amino terminal of the dipeptide derivative Fmoc-Arg(Pmc)-Ala-O-*t*Bu was carried out by treating the protected peptide (100 mg) with freshly distilled DMF (4.5 mL) and piperidine (0.5 mL) for 20 min. After removal of the solvent mixture by evaporation under vacuum, the residue was dissolved in chloroform and chromatographed on silica gel. The protecting group was eluted using chloroform, while using a mixture of chloroform-methanol 100:1 (v/v) it was possible to separate a small fraction of unreacted, protected peptide. The unprotected peptide H−Arg(Pmc)-Ala-O-*t*Bu was eluted with methanol (yield 60%).

The condensation between protohemin chloride and the dipeptide derivative was carried out as follows. A solution of protohemin chloride (74 mg, 0.11 mmol), HOBt (54 mg, 0.7 mmol), HBTU (43 mg, 0.11 mmol), and triethylamine (63 $\mu$L) in freshly distilled DMF (6.0 mL) was stirred for 15 min. Then, the dipeptide derivative H-Arg(Pmc)-Ala-O-*t*Bu (43 mg, 0.076 mmol) was added and the mixture was reacted overnight under stirring at r.t.; an aluminum foil was used to protect the flask from light. The mixture was then evaporated to dryness at r.t. under vacuum. The residue was treated several times with petroleum ether, and subsequently with water, and centrifuged or filtered each time in order to completely remove traces of DMF and at least part of the organic reagents. Then, it was dissolved in chloroform and chromatographed on a silica gel column (4.5 × 55 cm) which was also kept protected from light. Using chloroform as eluent, HOBt and other organic products such as tetramethylurea are eluted. With a mixture of chloroform-methanol 5:1 (v/v) successive elution of the bis-condensated ($R_f$ = 0.68) and the mono-condensated ($R_f$ = 0.47)

hemin-dipeptide derivatives occurs. Unreacted protohemin sticks on the column and can be removed by elution with methanol. Removal of the Pmc and O-*t*Bu protecting groups was carried out dissolving the mono-condensated hemin-dipeptide derivative in trifluoroacetic acid (5 mL) and adding thioanisole (0.25 mL) and water (0.25 mL). After 3 h, the mixture was evaporated to dryness under vacuum. The oily residue was treated several times with diethyl ether, that was discarded by decantation, and finally by filtration, giving the HM-RA complex as a dark powder. The product was characterized by FABMS spectrometry. The absorption maxima for the pyridine hemochrome derivative of HM-RA occur at 414, 520, and 550 nm. This derivative was prepared according to ref. *33*.

*Reconstitution of Myoglobin*. Apomyoglobin was prepared by the standard acid/2-butanone method (*34*). A stoichiometric amount of HM-RA or HM-H complex in methanol (about $10^{-3}$ M) was added to an apomyoglobin solution ($5.4 \times 10^{-4}$ M) in 10 mM phosphate buffer pH 5.0 (2.0 mL) cooled in an ice bath. After incubation for 10 min, the solution was transferred into a dialysis membrane kept in a large vessel containing 10 mM phosphate buffer pH 5.0 (300 mL) under slow stirring at 4 °C. Dialysis was continued for 2 days in these conditions, with three changes of the buffer per day, followed by additional dialysis against 10 mM phosphate buffer at pH 6.0 for another day. The optical spectra of the reconstituted proteins show Soret bands at 408 nm, with a ratio of $A_{408}/A_{280} \geq 2.4$, for Mb-RA, and 412 nm, with $A_{412}/A_{280} \geq 3.5$, for Mb-H. All the above manipulations were carried out in a cold room at 4 °C. The molar extinction coefficient of the electronic absorption of Mb-H was determined with the pyridine hemochromogen method (*33*), but that of Mb-RA could not be determined with this method, since the pyridine hemochrome spectrum of Mb-RA (absorption maxima at 414, 520, and 550 nm), like that of HM-RA, differs from that of heme *b* containing proteins. The extinction coefficients of the optical bands of the Fe(III) derivative (resting form) of Mb-RA were thus obtained by determination of the iron concentration, using atomic absorption spectroscopy, in a solution of known absorbance. Calibration of the instrument was performed using Mb solutions of known concentration as standards.

*Spectra of Mb, Mb-H and Mb-RA.* All absorption spectra of protein derivatives were recorded in 200 mM phosphate buffer, pH 6.0. The iron(II) species were obtained upon reduction of the iron(III) derivatives of the proteins with sodium dithionite under anaerobic conditions. The carbon monoxide adducts were obtained by bubbling CO into the solutions of the iron(II) species. Adding dioxygen to the Fe(II)-CO species gives rise to the formation of the Fe(II)-$O_2$ derivative in the case of Mb and Mb-H, while Mb-RA forms the iron(III) species. The Fe(II)-$O_2$ adduct of Mb and Mb-H could also be obtained by treating the protein with an excess of sodium ascorbate, in the presence of dioxygen, and allowing the solution to stand for 1 h. In the case of Mb the adduct is stable for hours, while with Mb-H it undergoes a slow bleaching of the heme chromophore. The incubation of Mb-RA with sodium ascorbate does not lead to the dioxygen adduct but produces heme degradation.

*NMR Spectra.* The proton NMR spectra were recorded on protein solutions of final concentrations between 0.1 and 1 mM in 100 mM phosphate buffer, pH 5.5, prepared in 10% $^2H_2O$/90% $H_2O$. The $H_2O$ resonance was reduced by presaturating its signal for 300 ms. For the high-spin Mb and Mb-H derivatives and for the Mb-imidazole adduct, obtained adding an excess of the ligand to the protein, 20K transients were collected with a 80 000 Hz (200 ppm) spectral width and using 64K data points. The signal-to-noise ratio was enhanced by an exponential apodization of 20 Hz. The spectra of the low-spin Mb-$CN^-$ and Mb-H$-CN^-$ adducts, obtained after the addition of excess KCN directly in the NMR tube containing the protein, were recorded collecting 4K transients with a spectral width of 24 000 Hz and 64K data points. The exponential apodization was of 10 Hz.

*Kinetics.* All kinetic experiments were performed in 200 mM phosphate buffer, pH 6.0 at 25.0 ± 0.1 °C, using a thermostated and magnetically stirred 1-cm path-length cell. The catalytic oxidation of phenols to dimerization products by hydrogen peroxide in the presence of Mb, and freshly prepared Mb-H or Mb-RA was followed spectrophotometrically by measuring the increase in absorbance at 300 nm in the initial phase of the reaction. The $H_2O_2$ concentrations of dilute solutions were determined by observing the formation of the $ABTS^{\bullet+}$ radical cation after reaction of the peroxide with an excess of ABTS in the presence of 40 nM of HRP at pH 7.0, using $\epsilon_{ABTS^{\bullet+}} = 1.47 \times 10^4$ $M^{-1}$ $cm^{-1}$ at 660 nm (*35*). The reactions were started by adding the $H_2O_2$ solution to the solution containing phenolic substrate and protein to a final volume of 1.6 mL. To reduce the noise in the absorbance readings, the differences in the absorbance between 300 and 500 nm, where the absorption of reagents and products is negligible, were monitored. The initial rates were taken from the first few seconds (typically 5−10 s) of the reactions. In preliminary experiments, the linearity between the oxidation rates of the phenolic substrates and catalyst concentrations was established. Relatively high concentrations of the phenols (solubility limited at 1.5 mM for L- and D-tyrosine, 3.5 mM for all the others) and hydrogen peroxide (8.7 mM) were used while that of the protein catalysts spanned from 0 to 1.5 $\mu$M. The noncatalytic reaction was often not negligible, so correction of the rate was necessary in order to obtain the real effect of the catalyst on the reaction rate. The study of the dependence of the rate on hydrogen peroxide concentration was performed using Mb (1.5 $\mu$M), Mb-RA (0.25 $\mu$M), or Mb-H (1.0 $\mu$M) as catalyst, varying the oxidant from 0.05 to 60 mM and keeping constant the substrate (1.5 mM for L- and D-tyrosine, while the other substrates were at 50 mM). Conversion of rate data from absorbance per seconds units into moles/L per second was effected using the difference in molar extinction coefficient between the mixture of dimeric products and the phenolic substrates at 300 nm: $\Delta\epsilon = 1460$ $M^{-1}$ $cm^{-1}$ for tyramine, $\Delta\epsilon = 1950$ $M^{-1}$ $cm^{-1}$ for *p*-hydroxyphenyl propionic acid, $\Delta\epsilon = 2350$ $M^{-1}$ $cm^{-1}$ for *p*-cresol, and $\Delta\epsilon = 1350$ $M^{-1}$ $cm^{-1}$ for L- and D-tyrosine. These $\Delta\epsilon$ values are pH dependent and were determined by enzymatic oxidation of phenolic substrates by horseradish peroxidase and hydrogen peroxide in phosphate buffer pH 6.0 following a procedure reported previously by us (*36*).

The kinetic experiments at variable substrate concentration were performed using constant protein (1.5 $\mu$M for Mb, 1.0 $\mu$M for Mb-H, and 0.25 $\mu$M for Mb-RA) and oxidant concentrations, and varying the concentration of the substrate: tyramine from 0.1 to 43 mM, $[H_2O_2] = 42$ mM;

*p*-hydroxyphenyl propionic acid from 0.2 to 70 mM, [$H_2O_2$] = 20 mM; *p*-cresol from 0.2 to 80 mM, [$H_2O_2$] = 20 mM; L- and D-tyrosine from 0.1 to 1.5 mM, [$H_2O_2$] = 4 mM. Using Mb or Mb-H as catalysts with tyramine and L- and D-tyrosine, and Mb-H with *p*-cresol, the reaction rates showed substrate saturation behavior. The kinetic parameters $k_{cat}$ and $K_M$ were calculated through the fitting of the rate vs substrate concentration data according to classical Michaelis−Menten treatment. Using Mb-RA as catalyst with all the substrates and Mb with *p*-cresol, at phenol concentration above 1 mM, the substrate oxidation rates depend linearly on the peroxide concentration. The oxidation of *p*-hydroxyphenyl propionic acid by Mb or Mb-H follows a biphasic behavior that can be accounted for considering the existence of two consecutive binding interactions of the substrate. The data could be fitted according to the following equation (see Supporting Information):

$$r = \frac{\frac{k_1[S]}{K_{D1}} + \frac{k_2[S]^2}{K_{D1}K_{D2}}}{1 + \frac{[S]}{K_{D1}} + \frac{[S]^2}{K_{D1}K_{D2}}}$$

where S represents the substrate, $K_{D1}$ and $K_{D2}$ the two dissociation constants characterizing the interaction, and $k_1$ and $k_2$ the rate contsnts for the oxidation of the protein-bound substrate in the mono and bis adduct, respectively.

The determination of the second order catalytic constant in the reaction of Mb or Mb-H with hydrogen peroxide to form the ferryl active species was performed by monitoring the spectral changes that occur upon addition of the oxidant to the protein. Using the stopped-flow technique and analyzing only the first few seconds of the reaction, the protein degradation occurring during the measurements can be neglected. In these experiments the concentration of Mb or Mb-H was 7 $\mu$M while that of the oxidant was changed from 25 to 200 $\mu$M. The kinetics of formation of the protein active species was analyzed by monitoring the absorbance changes between 408 and 428 nm for Mb and between 410 and 426 nm for Mb-H. In the case of Mb-RA, an estimate of this rate constant was obtained from the kinetics of oxidation of the phenolic substrates by hydrogen peroxide, from the linear part of the plots of rates vs [$H_2O_2$] at low oxidant concentrations.

*Binding Experiments.* The equilibrium constants for the binding of azide and imidazole to Mb and freshly prepared Mb-H and Mb-RA were determined by spectrophotometric titrations in 200 mM phosphate buffer pH 6.0 at 25 ± 0.1 °C using a thermostated optical cell (1 cm). A few microliters of concentrated ligand solutions were added to a 1.6-mL solution of the protein (5−10 $\mu$M) under stirring. Difference spectra of protein−ligand vs protein solution were taken after correction for dilution after each addition of the titrant. The binding constants and stoichiometry of the complexes were determined as described previously (*37*) or using the high affinity binding equation and the two consecutive binding equations described in the Supporting Information, according to the needs.

*MM and MD Calculations.* The X-ray structure of horse heart myoglobin was obtained from the Brookhaven Protein Data Bank. All calculations were carried out using the InsightII/Discover software (*38*) while home-developed programs were used for MD trajectory analysis. The basic structural information of the pdb file was completed according to the following procedure: (i) missing hydrogens were added to the protein, according to standard geometry rules; (ii) the geometry of the protein side chains was optimized keeping the protein backbone tethered; in a subsequent step, (iii) only the α-carbons of the peptide chain were restrained; and, finally (iv) a fully unconstrained accurate optimization (largest gradient component smaller than 0.01 kcal Å$^{-1}$) was performed on the whole system. Molecular dynamics were computed at 300 K for 250 ps starting from the optimized structure. The system was gradually heated at 300 K during the first 50 ps of simulation and the last 200 ps were used in the evaluation of time averaged properties. The final averaged structures have been optimized by MM to compare structures and energies of the different adducts. The MM force field used is a modification, specifically worked out for hemoproteins (*39*), of the Consistent Valence Force Field (CVFF) (*40*).

Calculations on reconstituted Mbs were performed including the hypothetical protein resulting from reconstitution of apoMb with the hemin complex HM-His-Ala (Mb-HA). By the comparison between Mb-H and Mb-HA we wanted to assess whether the terminal alanine residue plays any role in the apoprotein−cofactor interaction. Eight different initial reconstituted protein structures were used for the computational investigation. These correspond to the various reconstitution modes of the modified hemin complexes outlined in Scheme 2. In the first and second structure (A and B) the

Scheme 2

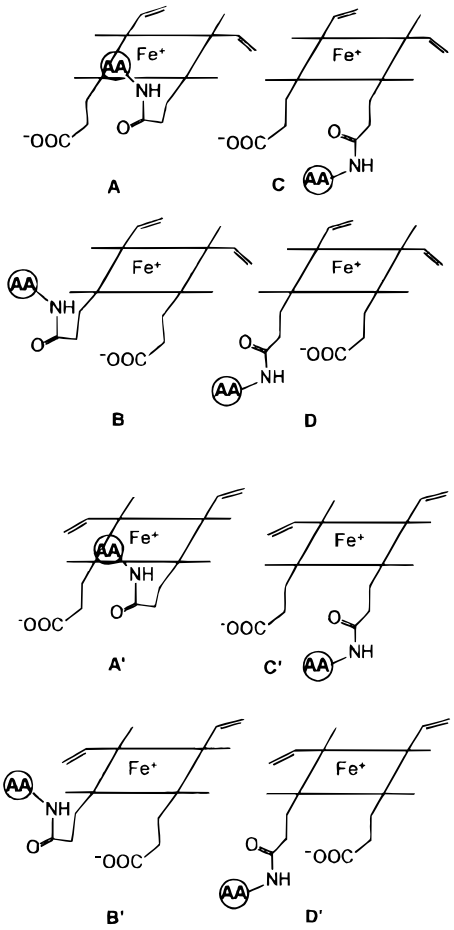

Table 1: Spectral Properties of Myoglobin Derivatives in 200 mM Phosphate Buffer, pH 6.0[a]

| derivative | Soret, nm ($\epsilon$, $mM^{-1}$ $cm^{-1}$) | visible, nm ($\epsilon$, $mM^{-1}$ $cm^{-1}$) | | |
|---|---|---|---|---|
| Mb: Fe(III) | 410 (160) | 504 (13.0) | $550^{sh}$ (7.0) | 632 (3.8) |
| Fe(III)-$CN^-$ | 424 (118) | 542 (14.0) | | $566^{sh}$ (12.0) |
| Fe(II) | 434 (110) | | 558 (12.0) | |
| Fe(II)-CO | 424 (176) | 540 (14.0) | | 572 (12.3) |
| Fe(II)-$O_2$ | 414 (100) | 542 (9.4) | | 580 (9.4) |
| Mb-RA: Fe(III) | 408 (115) | 528 (12.0) | $564^{sh}$ (9.0) | 620 (4.0) |
| Fe(III)-$CN^-$ | 412 (130) | 534 (16.0) | | $566^{sh}$ (12.0) |
| Fe(II) | 422 (100) | $532^{sh}$ (10.0) | | 550 (14.0) |
| Fe(II)-CO | 416 (150) | 532 (14.5) | | $560^{sh}$ (12.0) |
| Fe(II)-$O_2$ | nd | nd | | nd |
| Mb-H: Fe(III) | 412 (133) | 528 (11.0) | $566^{sh}$ (7.5) | 632 (3.0) |
| Fe(III)-$CN^-$ | 422 (110) | 542 (11.0) | | $566^{sh}$ (9.0) |
| Fe(II) | 434 (120) | | 560 (15.0) | |
| Fe(II)-CO | 424 (186) | 538 (15.0) | | 576 (15.2) |
| Fe(II)-$O_2$ | 416 (93.5) | 542 (11.7) | | 580 (11.2) |

[a] nd, not determinable.

His, His-Ala, or Arg-Ala groups were linked to the 6 and 7 propionate side chains of the porphyrin, respectively, with the substituent residue folded in order to stay in the distal side of the heme pocket. In the third and fourth structures (C and D) the His, His-Ala, or Arg-Ala groups were again linked to the two propionate side chains but they were oriented to stay outside the heme pocket. In these four orientations the heme ring was placed in the protein pocket with the vinyl groups oriented as in the X-ray structure of the native protein. However, upon reconstitution of the apoprotein, the heme group can enter the pocket upside-down and maintain the same orientation of the propionate side chains with respect to the protein surface. Therefore, at least in principle, other four initial starting structures are possible (A′, B′, C′, D′).

## RESULTS

*Synthesis of Modified Hemins and Reconstitution of apoMyoglobin*. The synthesis of the covalently modified protohemin complexes HM-H and HM-RA was performed following a route previously employed for the preparation of deuterohemin−peptide complexes (*22*−*24*). To introduce an arginine residue into HM, the dipeptide Arg-Ala was used, because condensation of the alanine residue represented a synthetically simpler method of protection of the arginine carboxyl group than esterification with the easily removable *tert*-butyl ester group. Condensation of protected His or Arg-Ala with HM occurs at the N-terminus of the residue and produces the monosubstituted hemin complexes as an isomeric mixture containing the substituent at position 6 or 7 of the porphyrin ring, together with the products of double condensation at both propionic acid side chains of the porphyrin. For Arg-Ala, the use of a ratio of peptide vs HM below the stoichiometric 1:1 value was found useful, to limit the formation of the bis condensation product. This improved the chromatographic separation of the desired product from the reaction mixture. Removal of the peptide protecting groups by mild acid treatment affords the hemin complex HM-RA. The FABMS spectrum of this product, obtained from a 3-nitrobenzyl alcohol matrix, shows the molecular ion cluster centered at *m*/*z* 1166, together with a smaller cluster of peaks corresponding to the hydroxide adduct of the complex.

The electronic spectra of HM-RA and HM-H in methanol show the typical absorption features for high-spin $Fe^{3+}$ species (*41*): Soret bands at 392 and 398 nm, $\beta$ bands at 490 and 492 nm, CT bands at 620 and 604 nm, respectively. The electronic spectrum of the pyridine hemochrome derivative of HM-RA (Soret band at 414 nm, $\beta$ band at 520 nm, $\alpha$ band at 550 nm) differs significantly from that of protoheme (*33*). Probably, at basic pH the deprotonated arginine guanidinium group competes with pyridine in coordinating to one of the iron sites.

For reconstitution of apomyoglobin with HM-RA several attempts had to be carried out, taking into account the very low solubility of the hemin complex in neutral aqueous buffer and the impractical use of the standard procedure based on dissolution of the cofactor in alkaline solution, and reconstitution in neutral medium (*28*), due to the possible racemization or cleavage of the peptide. Since the solubility of HM-RA is appreciable in methanol-aqueous buffer, pH 5.0, but reconstitution of apomyoglobin at this pH does not occur (or is very slow), we found that reconstitution could be carried out by slowly rising the pH of the buffer solution from pH 5.0 to 6.0. At pH closer to neutrality, or by a rapid rise in pH from 5.0 to 6.0, precipitation of the hemin complex or aggregates of this with apomyoglobin or reconstituted Mb-RA protein occurs. Reconstitution of Mb with HM-H was carried out in the same conditions. In both cases, reconstitution of apomyoglobin could be followed by the shift of the Soret peak of the free hemins in the buffer (below 400 nm) to 408 nm (Mb-RA) or 412 nm (Mb-H). The ratio of the Soret absorbance to the protein absorbance (at 280 nm) in Mb-RA and Mb-H is lower than for native Mb. This difference is due to the lower molar absorbance of the Soret band (Table 1 and vide infra). There is no evidence for the presence of appreciable amounts of apomyoglobin in the reconstituted protein solutions. In any case, the effect of traces of residual apomyoglobin in the catalytic and binding studies performed on Mb-RA and Mb-H is negligible.

*Characterization of Mb-RA and Mb-H*. While the electronic spectra of resting Mb-RA and Mb-H differs only slightly from that of ferric Mb in the Soret region [a small shift of ±2 nm from 410 nm in the native protein (*34*)], in the visible region the spectra of the two reconstituted proteins are different (Table 1). While the bands at 504 and 632 for

Table 2: Secondary Structure Calculations from the CD Spectra for Mb, Mb-H, and Mb-RA in 200 mM Phosphate Buffer, pH 6.0

| | Mb | Mb-H | Mb-RA |
|---|---|---|---|
| α-helix | 46.1 | 45.2 | 45.5 |
| turn | 4.1 | 1.5 | 0.0 |
| *β*-sheet | 21.1 | 23.2 | 26.3 |
| coil | 28.7 | 30.1 | 28.1 |

metMb are typical for a high-spin ferric iron with water as the sixth ligand (*5*, *41*), the absorptions at 528 and near 565 nm (the $Q_v$ and $Q_0$ bands, respectively) in the reconstituted proteins indicate the presence of a low-spin iron(III) center. Though, a fraction of high-spin species is still present in solution, as indicated by the CT band at ∼620 nm. These spectral characteristics are indicative of the presence of both high-spin and low-spin $Fe^{3+}$ species in Mb-RA and Mb-H. Similar spectra were observed for the Val68His mutant of myoglobin (*6*), where the presence of a further histidine residue in the distal site that can coordinate to the iron gives rise to a thermal high-spin/low-spin equilibrium. Upon reduction, the electronic spectrum of Mb-H becomes quite similar to that of Mb, with a high-spin ferrous center, while that of Mb-RA indicates a six-coordinate, low-spin form (*42*). Therefore, the reduced form of Mb-RA is also reminiscent of the Val68His mutant of myoglobin (*6*), with UV−vis spectral properties similar to those of cytochrome $b_5$, where the iron center is bound to two histidine residues (*43*). Interestingly, both Mb-RA derivatives that should contain a linearly bound diatomic, i.e., Fe(III)-$CN^-$ and Fe−CO, exhibit a blue shifted Soret band, which seems to indicate a distorted coordination of the axial ligand.

The CD spectra of Mb-RA and Mb-H show shifted Soret peaks with reduced CD activity (395 nm, $\Delta\epsilon$ + 8.5 $M^{-1}$ $cm^{-1}$; 415 nm, $\Delta\epsilon$ + 18.6 $M^{-1}$ $cm^{-1}$, respectively) with respect to ferric Mb (406 nm, $\Delta\epsilon$ + 21.3 $M^{-1}$ $cm^{-1}$), in phosphate buffer, pH 6.0. The reduced CD intensity reflects the fact that the reconstituted proteins are heterogeneous from the point of view of cofactor reconstitution mode, since it is known that disordered heme orientation within the protein reduces or even cancels the Soret CD (*44*). The CD spectra of Mb-RA and Mb-H in the peptide, far-UV region are very similar to that of native Mb, indicating that the secondary structure is essentially maintained in the reconstituted proteins (Table 2).

For Mb-H a direct observation of the composition of the reconstituted protein in terms of cofactor reconstitution mode could be obtained by NMR. Solubility problems prevented to obtain solutions of Mb-RA of sufficient concentration to perform reliable NMR studies. Figure 1, curves A−C, compares the low field portion of the NMR spectrum of Mb-H at pH 5.5 with those of Mb and the adduct Mb-imidazole in the same conditions. Freshly prepared Mb-H appears to be present in solution as a mixture of four isomers, two in a high-spin state and two in a low-spin state. The high-spin isomers are characterized by the peaks at about 53 and 72 ppm, attributable to heme methyls at position 1 and 3, respectively, which are split in two components, and by the four main peaks between 80 and 92 ppm, where the resonances of the heme methyl groups at position 5 and 8 of Mb occur (*45*). However, the most prominent features occur in the intermediate field region of the spectrum were a couple of intense peaks at 30.5 and 45.5 ppm and a couple

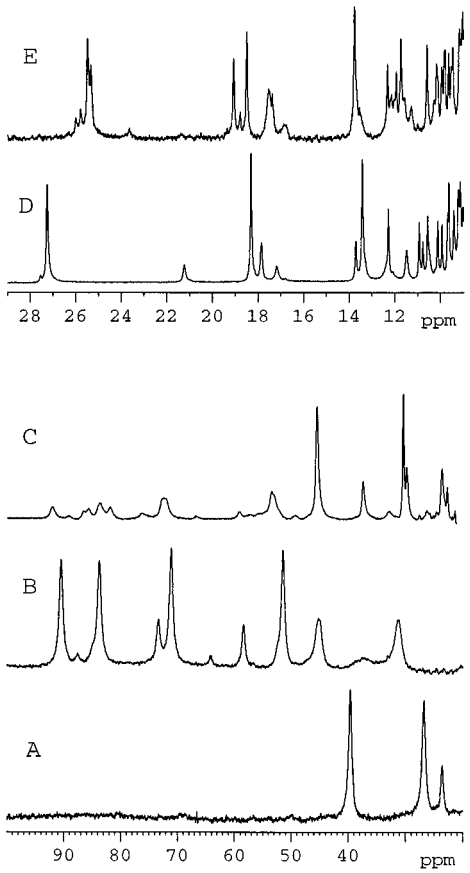


FIGURE 1: Downfield portion of the 400 MHz proton NMR spectra of Mb and Mb-H derivatives recorded in 0.1 M phosphate buffer, pH 6.0 containing 10% $^2H_2O$ at 25 °C. (A) Mb-imidazole complex, (B) Mb, (C) Mb-H, (D) Mb-$CN^-$ adduct, (E) Mb-H-$CN^-$ adduct.

of other peaks of notable intensity at 37.5 and 30 ppm are observed. Due to their high intensity, the protons of the propionate chains or the vinyl groups cannot account for these signals. The comparison with the spectrum of the Mb-imidazole adduct suggests that the Mb-H solution also contains two species with an imidazole bound at the sixth iron position. The NMR peaks in the range 30−50 ppm bear close resemblance also with those characterizing Mb variants existing as spin equilibria, like the Val68His mutant (*6*), confirming our inference from the UV−vis spectral data of the reconstituted Mbs.

It is interesting to note that the NMR spectrum of Mb-H changes very slowly with time indicating that the isomeric mixture undergoes a slow equilibration reaction. In the spectrum recorded on Mb-H incubated for 2 months after reconstitution, both the number of peaks in the low and mid field regions decreases with respect to a freshly prepared sample and only one high-spin species and one species with imidazole bound at the sixth iron position are observed (data not shown). The NMR spectrum of freshly prepared Mb-H becomes simpler after addition of cyanide (Figure 1E), since all isomers are converted into their low-spin cyanide form. The presence of four isomers is still evident from the comparison with the spectrum of Mb-$CN^-$ (Figure 1D). In particular, the signal near 27 ppm, attributable to the heme 5-methyl group in Mb-$CN^-$ (*45*) appears split into four peaks in Mb-H−$CN^-$.

*Ligand Binding Studies*. To assess the effect of the chemical modification of the protein-bound hemin on the

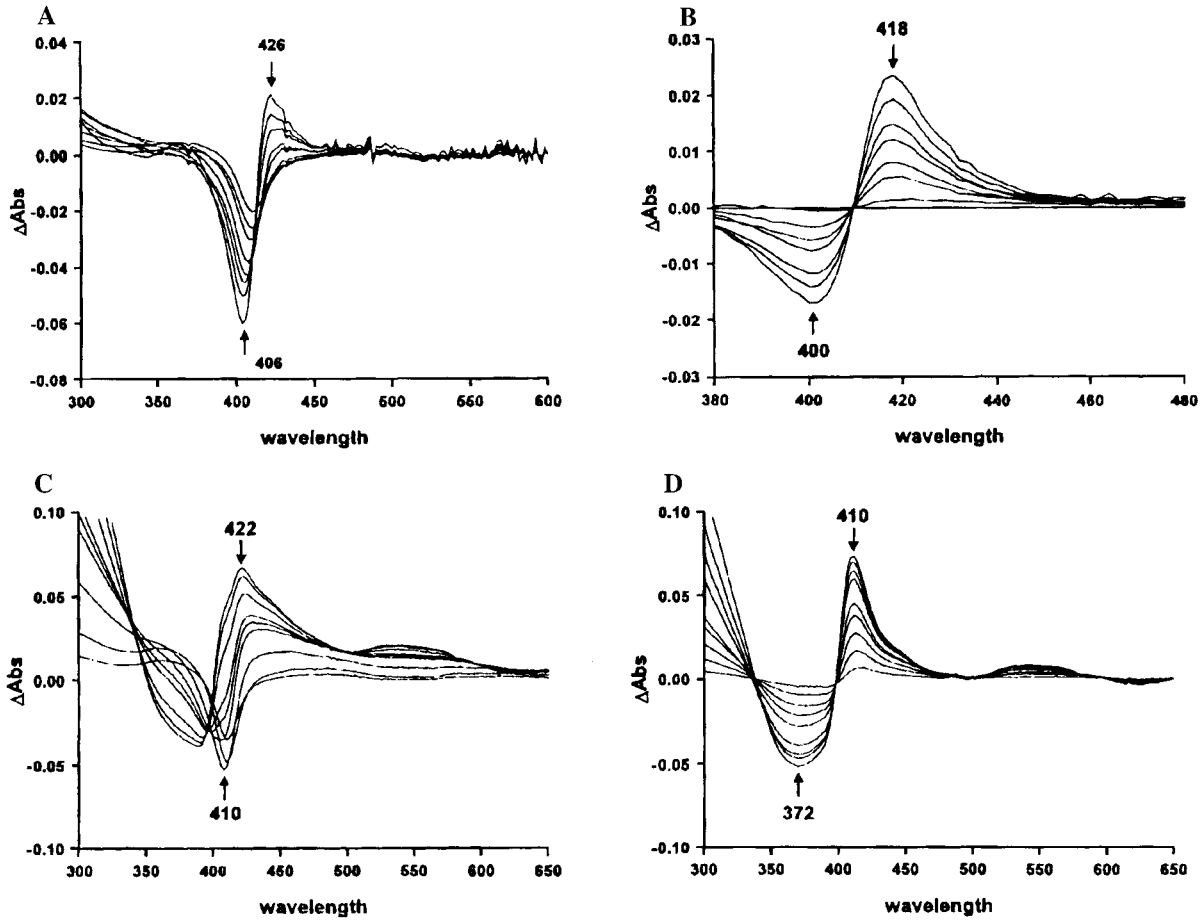


FIGURE 2: Titration of Mb-RA (3 $\mu$M) with azide and imidazole in phosphate buffer 200 mM, pH 6.0, 25 °C. (A) Difference spectra at various additions of $N_3^-$; (B) difference spectra with respect to Mb-RA bound to one azide anion ($[N_3^-] \approx 25$ mM), at various additions of $N_3^-$; (C) difference spectra at various additions of imidazole; (D) difference spectra with respect to Mb-RA bound to one imidazole ([Im] $\approx$ 0.5 mM), at various additions of the ligand.

accessibility to the sixth iron coordination position, comparative binding studies of the exogenous ligands azide and imidazole to Mb, and freshly prepared Mb-H and Mb-RA were performed. The titration experiments were carried out in 200 mM phosphate buffer, pH 6.0 at 25 ± 0.1 °C, following the change in intensity and the shift to lower energy of the Soret band on adduct formation. In the imidazole or azide binding experiments to Mb and Mb-H, isosbestic points were maintained throughout the titrations and difference spectra were used for calculation of binding constants. The final spectra are the same as those reported previously for ferric Mb (*34*), and the stoichiometry of binding was found 1:1 in all cases. The affinity of Mb for azide and imidazole found here, and measured by the constants $K = (4.5 \pm 0.1) \times 10^4$ $M^{-1}$ and $20 \pm 2$ $M^{-1}$, respectively, agrees with literature data (*34, 46*). For Mb-H the $K$ values are somewhat different: $(3.0 \pm 0.1) \times 10^4$ $M^{-1}$ for azide and $43 \pm 2$ $M^{-1}$ for imidazole. Mb-RA behaves in a different way, since the binding of both ligands occurs in two consecutive steps, with only small perturbations in the UV spectrum. The first ligation to reconstituted protein occurs with a slight decrease in the Soret band intensity, while in the second step the band shifts to lower energy (Figure 2). Both the constants for the two equilibria could be obtained: $K_1 = (3.0 \pm 0.8) \times 10^5$ $M^{-1}$ and $K_2 = (7 \pm 1) \times 10^2$ $M^{-1}$ for azide, and $K_1 = (4.1 \pm 1.2) \times 10^3$ $M^{-1}$ and $K_2 = 45 \pm 8$ $M^{-1}$ for imidazole.

Scheme 3

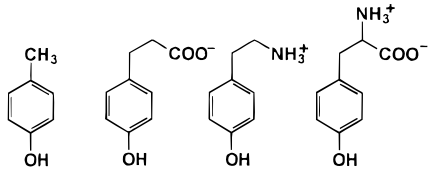


*Kinetic Studies*. For the assay of the catalytic activity of reconstituted Mb-H and Mb-RA proteins, the oxidation of representative phenolic substrates by hydrogen peroxide was chosen. Phenols are typical substrates for peroxidases (*47*−*49*), and their catalytic oxidation by these enzymes has been studied in detail by our group (*36*, *50*, *51*). The phenols used in the present investigation are *p*-cresol, *p*-hydroxyphenyl propionic acid, tyramine, and L- and D-tyrosine, which carry no charge, a negative charge, a positive charge, or both, respectively, on the substituent to the phenol ring (Scheme 3). The catalytic reaction converts the substrates to phenoxy radicals, which evolve independently of the catalyst to form two dimeric products in the initial phase (the α,α dimer and the Pummerer ketone) (*36*), and subsequently a mixture of oligomeric products. In the initial experiments, the dependence of the reaction rate on the concentration of the protein catalyst was assessed for each substrate. A linear dependence was found in all cases. Catalysis by Mb in the reaction of phenols with peroxides is thought to occur through a catalytic cycle that resembles that of peroxidases. After reaction with

Table 3: Kinetic Parameters for the Catalytic Oxidation of Phenols by Hydrogen Peroxide in 200 mM Phosphate Buffer, pH 6.0, in the Presence of Mb and Mb-H

| | Mb | | | Mb-H | | |
|---|---|---|---|---|---|---|
| substrate | $k_{cat}$ ($s^{-1}$) | $K_M$ (mM) | $k_{cat}/K_M$ ($M^{-1}$ $s^{-1}$) | $k_{cat}$ ($s^{-1}$) | $K_M$ (mM) | $k_{cat}/K_M$ ($M^{-1}$ $s^{-1}$) |
| tyramine | $0.36 \pm 0.02$ | $15 \pm 2$ | $24 \pm 2$ | $0.96 \pm 0.03$ | $6.0 \pm 0.8$ | $158 \pm 16$ |
| L-tyrosine | $0.052 \pm 0.02$ | $0.36 \pm 0.04$ | $140 \pm 10$ | $0.26 \pm 0.01$ | $0.39 \pm 0.04$ | $660 \pm 50$ |
| D-tyrosine | $0.047 \pm 0.01$ | $0.26 \pm 0.02$ | $180 \pm 10$ | $0.26 \pm 0.01$ | $0.39 \pm 0.06$ | $670 \pm 80$ |
| *p*-cresol | *a* | *a* | | $13.4 \pm 0.6$ | $3.0 \pm 0.5$ | $4500 \pm 500$ |
| *p*-hydroxy-phenyl propionic acid[b] | $k_1 = 0.09 \pm 0.05$<br>$k_2 = 2.3 \pm 0.3$ | $K_{D1} \approx 0.1$<br>$K_{D2} = 70 \pm 20$ | | $k_1 = 0.35 \pm 0.15$<br>$k_2 = 40 \pm 10$ | $K_{D1} \approx 0.1$<br>$K_{D2} = 300 \pm 100$ | |

[a] See text. [b] The kinetic parameters referring to the biphasic behavior observed in the oxidation of this substrate are defined in the Experimental Procedures.

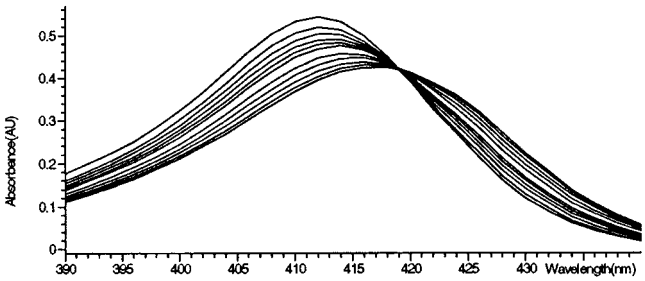


FIGURE 3: Rapid scan (0−26 s) of the reaction between Mb-H (7 $\mu$M) and hydrogen peroxide (30-fold excess) in 100 mM phosphate buffer, pH 6.0, at 25 °C.

$H_2O_2$ a two-electron oxidized, iron-oxo protein radical intermediate is formed, with the radical probably located on a protein tyrosine residue (*52*−*54*). This species is very reactive and reacts with the substrate forming the iron-oxo adduct, which in turn oxidizes another substrate molecule, restoring the iron(III) form of the protein. The comparison of the activity of Mb with those of Mb-RA and Mb-H should be done by observing the dependence of the reaction on both hydrogen peroxide and phenol concentrations. The free HM-RA and HM-H complexes and simple (nonreconstituted) mixtures of these hemins and apomyoglobin are immediately and completely degraded by hydrogen peroxide in the reaction conditions (i.e., in the presence of phenol) even upon addition of imidazole.

The kinetics of formation of the active oxoferryl species by hydrogen peroxide could be determined for Mb and Mb-H by stopped-flow spectroscopy, while Mb-RA undergoes extensive degradation in the presence of excess hydrogen peroxide. In the former cases, the reaction with $H_2O_2$ is accompanied by a shift of the Soret band of the proteins to 418 nm (Mb-H) (Figure 3) and 420 nm (Mb) and a decrease of intensity. The kinetic constants ($k_1$) for the formation of these compound II-like intermediates (at pH 6.0) are $700 \pm 20$ $M^{-1}$ $s^{-1}$ for Mb and $900 \pm 50$ $M^{-1}$ $s^{-1}$ for Mb-H; the $k_1$ value found here for Mb is similar to that reported at pH 7.0 (*21*). An estimate of $k_1$ for Mb-RA was obtained from the kinetics of substrate oxidation at very low hydrogen peroxide concentration (see below).

Assuming that for Mb, Mb-H and Mb-RA, as for classical peroxidases (*47*, *48*, *55*), a simple bimolecular ping−pong mechanism is valid, the catalyst must react with hydrogen peroxide prior to the reaction with the phenol. The slower of the two processes is the rate determining step of the reaction. Thus, to observe the substrate dependence of the reaction rate it was necessary to determine the minimal concentration of oxidant which makes formation of the protein active intermediate a fast process. This avoids, at the same time, usage of an inconvenient excess of hydrogen peroxide, which may be harmful to the protein. The optimization of the oxidant concentration required in the kinetic experiments was obtained by studying the dependence of the reaction rate on peroxide concentration and maintaining fixed, and relatively high, that of each substrate. The resulting plots of rates vs oxidant concentration were found to be linear with all the substrates in the kinetic experiments performed with Mb-RA and in the oxidation of *p*-cresol with Mb. Using tyramine, *p*-hydroxyphenyl propionic acid, and L- or D-tyrosine the plots of rate vs $[H_2O_2]$ in the reactions catalyzed by Mb follow a hyperbolic behavior. The same behavior is observed in all catalytic reactions performed with Mb-H. The protein spectra recorded during turnover show that when the peroxide concentration is low (in the linear part of the plot of rate vs $[H_2O_2]$), the proteins are present in solution essentially in the native form. Thus, the slow step of the reaction is the active species formation. From the slope of the plot, an estimate of the second-order catalytic constant ($k_1$) for the reaction of the peroxide with Mb-RA was obtained. This value was found within the experimental error, independent of the substrate: $k_1 = 70 \pm 10$ $M^{-1}$ $s^{-1}$.

Using either Mb or Mb-H as catalysts and under saturating oxidant conditions the protein is present in its active form during turnover and the reaction rate is regulated by the interaction with the phenolic substrate (except for *p*-cresol with Mb). When the reaction rates were studied as a function of the substrate concentration, saturation behavior was observed. This indicates that binding of the phenolic compounds to the active form of the Mb catalyst is an essential step preceding electron transfer. Analysis of the rate data, in terms of the kinetic parameters $k_{cat}$ and $K_M$ (*56*) gave the values reported in Table 3. The rate data for the oxidation of *p*-hydroxyphenyl propionic acid with Mb and Mb-H had to be analyzed with a kinetic equation that takes into account the observed biphasic behavior (Table 3). The estimate of the first substrate dissociation constants ($K_{D1}$) in both cases is subject to a large uncertainty, because it refers to a high affinity equilibrium.

*MM and MD Calculations.* Molecular mechanics and dynamics simulations of the reconstituted Mb-RA, Mb-HA and Mb-H proteins starting with cofactor structures where the substituent attached to the propionate group is folded over the porphyrin plane (A, B, A′, B′) indicated that a severe modification of the structure of the protein active site takes place. This is due to steric clashing between the amino acids side chains linked to the porphyrin macrocycle and the amino acid residues forming the active site. In particular, the distal

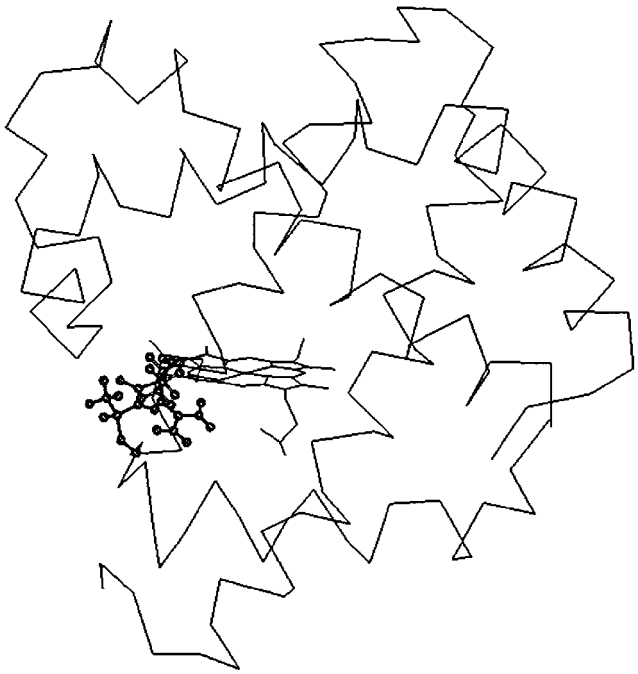

FIGURE 4: Structure of reconstituted myoglobin as obtained by averaging of MD trajectory starting from hemin structure D′. For the sake of clarity only the alpha-carbons of the protein, the hemin macrocycle and the Arg-Ala dipeptide (ball-and-stick representation) are shown.

pocket does not seem to be sufficiently large to favorably accommodate the His, His-Ala or Arg-Ala residues, at least in the conformation that these can assume when bound to the propionic acid chains. MM and MD calculations started with reconstituted Mb structures where the modified propionate extends outside the heme pocket (C, D, C′, D′) resulted in protein structures very similar to the native myoglobin structure. As an example, the structure of reconstituted myoglobin as obtained by averaging over the last 200 ps of molecular dynamics simulation starting from hemin structure D′ featuring the Arg-Ala group is shown in Figure 4. This indicates that the heme modification does not affect the tertiary structure of the protein, in agreement with the CD data. Therefore, this set of data suggests that the amino acids linked to the propionate side chain cannot adopt a favorable conformation within the heme pocket but will be oriented outside it, sampling the protein region corresponding to the small channel connecting the heme cofactor with the bulk solvent. However, slightly different results were obtained initializing the MM/MD runs with reconstituted protein structures (C, D, C′, D′) characterized by the latter arrangement of the propionate substituents. It has been shown that specific electrostatic interactions between the heme propionates and amino acids at the surface of the protein appear to be important in the stabilization of the bound porphyrin in myoglobin (*57*). In fact, analysis of the myoglobin X-ray structure indicates that the heme ring is linked to the protein by two specific electrostatic interactions. The carboxylate of propionate 6 interacts with the side chain of Lys45, whereas the carboxylate of propionate 7 interacts with the side chain of Ser92 and His97. Insertion of the modified hemins into the protein affects these interactions. In particular, in protein structures characterized by the heme-propionate substituent with orientations D and D′ the salt bridge established with the side chain of Lys45 cannot be maintained and the analysis of MD trajectory for these complexes indicate that this missing bond confers a greater mobility to the polypeptide segment Phe43−Lys47 making the protein active site more accessible to exogenous ligands and more prone to undergo a collapse of the distal helix. However, the Mb-H and Mb-HA derivatives are characterized (at least in most MD frames) by a hydrogen bond formed between the imidazole side chain of the modified cofactor and Asp44, making the protein active site slightly more rigid and therefore less prone to undergo the collapse of the distal active site. On the other hand, in protein-hemin complexes C and C′, the lost interaction is that between the carboxyl group of the propionate side chain with Ser92 and His97. However, in this case no important structural changes are observed in the distal side of the active site. It is also apparent that the presence of a terminal Ala residue on the cofactor side chain has no influence on the stereochemical characteristics of the reconstituted Mb.

In principle, the MM/MD investigation of reconstituted proteins characterized by heme groups with C, D, C′, and D′ arrangements could allow a quantitative comparison of the relative stability of these adducts. Even if the lack of explicit solvent molecules and the relatively short runs currently makes this analysis only qualitative, our results indicate that the optimized C′ and D′ adducts are always slightly more stable than the corresponding C and D forms, in agreement with experiments where it has been shown that the two positions for the heme, differing by 180° rotation about the $\alpha-\gamma$ meso axis, are equally populated soon after heme-apoprotein reconstitution, but their relative proportion becomes highly asymmetric (90:10) after equilibration (*58*). On the other hand, the relative energies of the optimized C′ and D′ species are so close that any definitive conclusion on their relative stability becomes somewhat speculative. However, even if more accurate models, including explicitly solvent molecules, are necessary to address this point, it is tempting to suggest, in light of these preliminary results, that both states could be appreciably populated at room temperature.

## DISCUSSION

Several factors contribute to the discriminating reactivity of peroxidases in peroxide activation reactions. Structural features shared by these enzymes include the hydrogen bonded, proximal histidine-aspartate couple, conferring anionic imidazolate character to the iron axial ligand, and the distal histidine and arginine residues, the first of which is hydrogen bonded to an asparagine, which are involved in the peroxide activation process and, possibly, compound I reduction (*1*−*4*, *25*, *59*−*61*). It is clearly difficult to introduce all these features into a different protein to model the catalytic activity of peroxidases. The approach currently followed in studies using myoglobin is based on replacement of specific amino acid residues by site-directed mutagenesis (*9*−*12*), but the results, in terms of rate enhancement in phenols oxidation reactions, are currently modest. In the present work we have explored the potential of an alternative approach, which is based on reconstitution of myoglobin with synthetically modified protohemins and can be eventually coupled with genetic engineering of the protein.

The modification of myoglobin by reconstitution with the modified heme prosthetic groups strongly affects the elec-

tronic, catalytic and binding properties of the protein. This indicates significant modification of the heme environment. The NMR spectra indicate that the reaction of apoMb with the isomeric mixture of HM-H (but probably the same occurs with HM-RA) gives initially rise to the formation of a mixture of four isomers, two with the heme methyl resonances at low field and the other two with signals at intermediate field. These isomers are represented in Scheme 2 as the forms C, D, C′, and D′. As shown by MM and MD calculations, the isomers D and D′ of Mb-H and Mb-RA lack the electrostatic interaction between the heme carboxylate and the protein Lys45 residue. This increases the mobility of the fragment Phe43−Lys47 containing the distal histidine and causes the possibility that the imidazole group can reach the iron, even though this coordination will occur with some strain. Since the NMR signals at intermediate field resemble those observed in the Mb-imidazole adduct (see Figure 1) and the Val68His mutant (*6*), they can be assigned to these D and D′ forms. Thus, the heme methyl signals at low field are connected with the fraction of C and C′ species present in solution. The species C and D can be converted to species D′ and C′, respectively, upon 180° heme rotation about the $\alpha-\gamma$ meso axis. The interconversion of the isomers occurs very slowly and requires incubation periods of the order of several weeks to be observed; however, after about two months the reorientation reactions reach an equilibrium and the isomeric mixture simplifies to only two forms. Since MM and MD calculations indicate that the two most stable species are C′ and D′, probably the species with NMR signals at low field is C′, while the other is D′. The presence of mixtures of species containing water or imidazole as sixth iron ligand in Mb-H and Mb-RA accounts for the observation of UV/Vis spectral characteristics of both low-spin and high-spin heme. The situation resembles that observed for the Val68His horse heart Mb mutant, where a bishistidine ligated protein is present (*6*), and the partially low-spin iron(III) form was explained by a weak iron-histidine bond. Collapse of the distal helix appears to be a somewhat more dramatic effect in Mb-RA, where also the reduced form maintains bis-histidine ligation, as in cytochrome $b_5$ (*43*). Strong ligands such as cyanide, azide, imidazole, or, in the reduced form, carbon monoxide can displace the distal His ligand, but in the Mb-RA forms Fe(III)-$CN^-$ and Fe(II)-CO, binding of the ligand appears to occur with some strain. This effect explains the impossibility to isolate the Fe(II)-$O_2$ derivative for Mb-RA and its limited stability in Mb-H. Probably, once the dioxygen adduct is formed, it releases a superoxide anion forming the iron(III) species. Then, superoxide dismutates in solution producing hydrogen peroxide. A similar mechanism is operative in the autoxidation of myoglobin (*62*) and here this is responsible for the heme degradation undergone by Mb-RA and Mb-H when incubated with ascorbate.

The observation of isosbestic points during this titration is particularly remarkable because of the 4-fold heterogeneity in the reconstituted protein. Thus, the imidazole group of the species containing six-coordinated iron(III) can be easily displaced by the ligand. The behavior of Mb-RA, though, shows that two azide ions or two imidazole molecules can bind to the protein. The first binding step is probably related to electrostatic interaction of the ligand with positively charged residues near the heme edge. This interaction could be connected with the arginine residue present in HM-RA but could also be present with Mb or Mb-H, where it may be hidden by the strong UV−vis changes caused by the interaction of the ligand with the heme. In the second binding step, the ligand interacts directly with the iron. For both reconstituted proteins, the affinity constant for imidazole is higher than that observed for Mb, while the affinity versus azide is reduced. Two different effects determine the value of these constants. The coordination of the exogenous ligand in Mb occurs on a high-spin protein with water as the sixth iron ligand. Instead, Mb-H and Mb-RA are in equilibrium between high-spin/low-spin forms; thus, the coordination of the ligand occurs with displacement of the distal ligand. This effect reduces the affinity constants. On the other hand, reconstitution of the protein with the modified heme opens the active site, allowing an easier access of the exogenous ligands. With the smaller ligand azide, the presence of a low-spin iron center overwhelms the effect of the increased accessibility of the iron; thus, the affinity constant is reduced. With the bulkier but stronger ligand imidazole, the relative importance of the two effects is reversed and the affinity toward Mb-H and Mb-RA becomes higher than that for Mb.

The catalytic cycle of peroxidases consists of three steps; the slowest step rules the activity of the enzyme. The high activity of peroxidases is connected to a very efficient activation process [the second-order constant for the reaction with hydrogen peroxide is in the order of $10^7$ $M^{-1}$ $s^{-1}$ (*47*, *63*)], but also with the presence of an accessible active site (relatively low $K_M$), where the substrate binds close to the porphyrin plane allowing a fast electron-transfer process (high $k_{cat}$). Usually, even at low oxidant concentration, the formation of the active species is a fast process and the slow step in the enzymatic reaction is reduction of compound II (*2*, *50*, *51*, *59*).

Myoglobin behaves in a different way. The amino acid backbone around the heme is not optimized for a fast reaction with hydrogen peroxide and this implies a low value for the rate of the active species formation ($k_1 = 700$ $M^{-1}$ $s^{-1}$). Moreover, the active site allows easy access of dioxygen but phenols bind in a position which is clearly not suited for a fast electron-transfer process. Thus, the $k_{cat}$ constant observed for Mb reactions (Table 3) are 2 orders of magnitude lower than those of peroxidases (*36*). The low $k_1$ value implies the need to use a large concentration of oxidant in order to make formation of the active species a fast step with respect to the restoration of the iron(III) form. With the uncharged and low potential substrate *p*-cresol, the oxidation process is fast and the reaction rate depends on the peroxide concentration, making impossible the evaluation of $k_{cat}$. Reconstition of Mb with HM-H increases the catalytic performance of the protein. Both $k_1$ (900 $M^{-1}$ $s^{-1}$) and $k_{cat}$ (Table 3) increase for Mb-H and this positive effect is often strengthened by a reduction in $K_M$, due to the better accessibility of the active site. The behavior of the two tyrosine enantiomers in the catalytic reactions is worth of note. These substrates have very low $K_M$ values and hence bind strongly to Mb (with a slight preference for the D isomer), probably for the presence of both cationic and anionic groups that can favorably interact with the hydrophilic active site periphery of the protein. Though, clearly the binding occurs with an arrangement in which the electron-transfer process from the phenol nucleus to the heme has a low efficiency. With Mb-H the $K_M$ values remain low

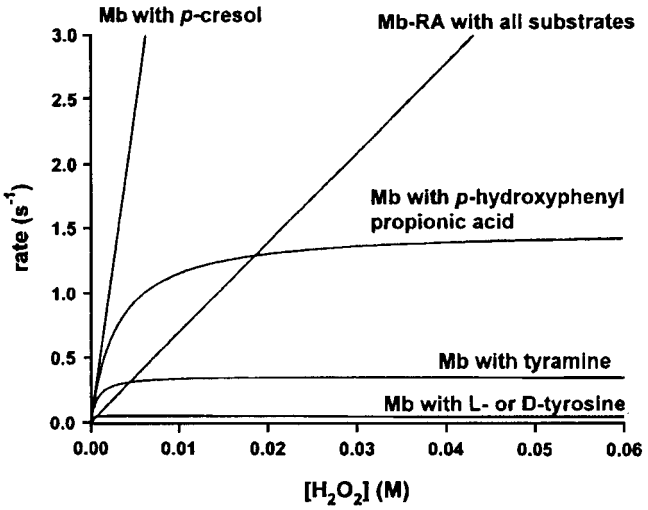


FIGURE 5: Dependence of the catalytic activity of Mb and Mb-RA (~1 $\mu$M) on peroxide concentration for the various substrates present in high concentrations (L- and D-tyrosine 1.5 mM, other phenols 50 mM) in 200 mM phosphate buffer, pH 6.0, at 25 °C.

(though the protein loses the ability to discriminate between L and D isomers) but $k_{cat}$ increases by about an order of magnitude.

Interestingly, the oxidation of *p*-hydroxyphenyl propionic acid, which is mostly anionic at pH 6.0, follows a biphasic behavior. Two substrate molecules bind close to the active site. The first one has high affinity but reacts slowly. Probably, this interaction involves the substrate carboxylate group and a positively charged residue close to the heme pocket, likely the same residue involved in the interaction with anionic ligands, but forces the phenol nucleus of the substrate in a position which is not suitable for a fast electron transfer process. With the second substrate binding interaction the phenol ring can approach the heme closer and the reaction occurs faster. Even though the kinetic constants are affected by a large degree of uncertainty, the data clearly indicate that Mb-H binds stronger and reacts faster with the substrate with respect to Mb in both the mono and bis ligated phases.

The catalytic activity of Mb-RA is characterized by a reduced $k_1$ value (7 times smaller than for Mb). This effect can be explained considering that the RA peptide chain of the modified hemin prefers to stay outside the surface in the reconstituted protein and thus has little role in the heterolytic cleavage of peroxide. At the same time, the presence of a fraction of protein in the six-coordinate, low-spin state requires that the binding of peroxide to the iron must occur with prior removal of the sixth ligand. On the other hand, Mb-RA exhibits high $k_{cat}$ values. Even if the $k_{cat}$ parameter cannot be determined, its higher value (with respect to that of Mb) can be argued by the rate values observed in the presence of high peroxide concentration. The increased $k_{cat}$ value is probably due to the fact that the presence of the modified heme opens the active site, allowing the approach of the substrate in a way that facilitates the electron transfer to form the phenoxy radical.The differences in the catalytic behavior of Mb and Mb-RA can be appreciated from the plots in Figure 5, where the activities of the two proteins at high substrate concentrations are reported as a function of $[H_2O_2]$. With the uncharged and easily oxidizable substrate *p*-cresol, the reactivity depends only on $k_1$, therefore Mb reacts faster than Mb-RA. The situation is different with the other substrates, since on increasing the peroxide concentration the reactivity order between the two proteins is reversed. This is particularly evident when the activities at about 50 mM peroxide concentration are considered. Mb-RA reacts 2-fold faster than Mb with the acid substrate, but the increase in activity raises to 10-fold with tyramine and to 70-fold with the two tyrosine isomers.

Thus, in conclusion, modification of the active site environment by reconstitution of Mb with modified heme derivatives markedly affects the binding and reactivity characteristics of the protein through two phenomena. The presence of a fraction of heme in a low-spin form, produced by collapse of the distal helix, reduces the direct accessibility to the iron center and hence has a negative effect on the catalytic process performed by the protein. On the other hand, the modified cofactor allows the substrates to bind more easily to the protein and with an arrangement that makes the electron transfer to the active species a (relatively) fast process. Since the importance of these effects depends on the nature of the chemically modified protohemin complex, reconstitution of the protein, eventually coupled with protein engineering, appears to open new perspectives in the attempts to obtain catalytically efficient myoglobin derivatives.

## SUPPORTING INFORMATION AVAILABLE

Derivation of the equations used for calculating the binding constants in a single and two consecutive ligand binding equilibria, and the reaction rates for two consecutive protein−substrate binding interactions. Plots of absorbance change for Mb-RA vs ligand (azide or imidazole) concentration and fitting with the equations for a single or two consecutive binding equilibria (Figure S1 and S2). Plots of absorbance change on binding of azide and imidazole to Mb-H (Figure S3 and S4). This material is available free of charge via the Internet at http://pubs.acs.org.

## REFERENCES

1. Ortiz de Montellano, P. R. (1987) *Acc. Chem. Res. 20*, 289−294.
2. Dawson, J. H. (1988) *Science 240*, 433−439.
3. Poulos, T. L. (1988) *Adv. Inorg. Biochem. 7*, 1−33.
4. Casella, L., and Colonna, S. (1994) in *Metalloporphyrins Catalyzed Oxidations* (Montanari, F., and Casella, L., Eds.) pp 307−340, Kluwer, Dordrecht.
5. Springer, B. A., Sligar, S. G., Olson, J. S., and Phillips, G. N., Jr. (1994) *Chem. Rev. 94*, 699−714.
6. Lloyd, E., Hildebrand, D. P., Tu, K. M., and Mauk, A. G. (1995) *J. Am. Chem. Soc. 117*, 6434−6438.
7. Van Dyke, B. R., Saltman, P., and Armstrong, F. A. (1996) *J. Am. Chem. Soc. 118*, 3490−3492.
8. Hirota, S., Li, T., Phillips, G. N., Jr., Olson, J. S., Mukai, M., and Kitagawa, T. (1996) *J. Am. Chem. Soc. 118*, 7845−7846.
9. Ozaki, S., Matsui, T., and Watanabe, Y. (1996) *J. Am. Chem. Soc. 118*, 9784−9785.
10. Ozaki, S., Matsui, T., and Watanabe, Y. (1997) *J. Am. Chem. Soc. 119*, 6666−6667.
11. Adachi, S., Nagano, S., Ishimori, K., Watanabe, Y., Morishima, I., Egawa, T., Kitagawa, T., and Makino, R. (1993) *Biochemistry 32*, 241−252.
12. Matsui, T., Nagano, S., Ishimori, K., Watanabe, Y., and Morishima, I. (1996) *Biochemistry 35*, 13118−13124.
13. Barrick, D. (1994) *Biochemistry 33*, 6546−6554.
14. Decatur, S. M., and Boxer, S. G. (1995) *Biochemistry 34*, 2122−2129.

15. Hildebrand, D. P., Burk, D. L., Maurus, R., Ferrer, J. C., Brayer, G. D., and Mauk, A. G. (1995) *Biochemistry 34*, 1997−2005.
16. Neya, S., Funasaki, N., and Imai, K. (1988) *J. Biol. Chem. 263*, 8810−8815.
17. Adams, P. A., Goold, R. D., and Thumser, A. E. (1989) *J. Chem. Soc., Faraday Trans. 1 85*, 3845−3852.
18. Hargrove, M. S., Barrick, D., and Olson, J. S. (1996) *Biochemistry 35*, 11293−11299.
19. Shulman, R. G., Wüthrich, K., Yamane, T., Antonini, E., and Brunori, M. (1969) *Proc. Natl. Acad. Sci. U.S.A. 63*, 623−628.
20. LaMar, G. N., Budd, D. L., Viscio, D. B., Smith, K. M., and Langry, K. C. (1978) *Proc. Natl. Acad. Sci. U.S.A. 75*, 5755−5759.
21. Hayashi, T., Hitomi, Y., Ando, T., Mizutani, T., Hisaeda, Y., Kitagawa, S., and Ogoshi, H. (1999) *J. Am. Chem. Soc. 121*, 7747−7750.
22. Casella, L., Gullotti, M., De Gioia, L., Monzani, E., and Chillemi, F. (1991) *J. Chem. Soc., Dalton Trans.* 2945−2953.
23. Casella, L., Gullotti, M., De Gioia, L., Bartesaghi, R., and Chillemi, F. (1993) *J. Chem. Soc., Dalton Trans*. 2233−2239.
24. Casella, L., Gullotti, M., De Gioia, L., Strini, A., and Chillemi, F. (1996) *Inorg. Chem. 35*, 439−444.
25. Finzel, B. C., Poulos, T. L., and Kraut, J. (1984) *J. Biol. Chem. 259*, 13027−13036.
26. Erman, J. E., Vitello, L. B., Miller, M. A., and Kraut, J. (1992) *J. Am. Chem. Soc. 114*, 6592−6593.
27. Rodriguez-Lopez, J. N., Smith, A. T., and Thorneley, R. N. F. (1996) *J. Biol. Inorg. Chem. 1*, 136−142.
28. Savenkova, M. I., Newmyer, S. L., and Ortiz de Montellano, P. R. (1996) *J. Biol. Chem. 271*, 24598−24603.
29. Tanaka, M., Ishimori, K., and Morishima, I. (1996) *Biochem. Biophys. Res. Commun. 227*, 393−399.
30. Nagano, S., Tanaka, M., Ishimori, K., Watanabe, Y., and Morishima, I. (1996) *Biochemistry 35*, 14251−14258.
31. Newmyer, S. L., and Ortiz de Montellano, P. R. (1996) *J. Biol. Chem. 271*, 14891−14896.
32. Monzani, E., Casella, L., Redaelli, C., Bassani, C., Santagostini, L., and Gullotti, M. (Submitted for publication).
33. Fuhrhop, J. H., and Smith, K. M. (1977) *Laboratory Methods in Porphyrins and Metalloporphyrins Research*, Elsevier, Amsterdam, The Netherlands.
34. Antonini, A., and Brunori, M. (1971) in *Hemoglobin and Myoglobin in Their Reactions with Ligands*, North-Holland, Amsterdam.
35. Adams, P. A. (1990) *J. Chem. Soc., Perkin Trans. 2*, 1407−1414.
36. Casella, L., Poli, S., Gullotti, M., Selvaggini, C., Beringhelli, T., and Marchesini, A. (1994) *Biochemistry 33*, 6377−6386.
37. Casella, L., Gullotti, M., Poli, S., Bonfà, M., Ferrari, R. P., and Marchesini, A. (1991) *Biochem J. 279*, 245−250.
38. Biosym/MSI, 9685 Scranton Road, San Diego, CA.
39. Angelucci, L., De Gioia, L., and Fantucci, P. (1993) *Gazz. Chim. Ital. 123*, 111−117.
40. Douber-Osguthorpe, P., Roberts, V. A., Osguthorpe, D. J., Wolff, J., Genest, A. T., and Hagler, A. T. (1988) *Proteins: Struct., Funct., Genet. 4*, 31−38.
41. Owens, J. W., and O′Connor, C. J. (1988) *Coord. Chem. Rev. 84*, 1−45.
42. Miller, M. A., Coletta, M., Mauro, J. M., Putnam, L. D., Farnum, M. F., Kraut, J., and Traylor, T. G. (1990) *Biochemistry 29*, 1777−1791.
43. Ozols, J., Strittmatter, P. (1964) *J. Biol. Chem. 239*, 1018−1023.
44. Aojula, H. S., Wilson, M. T., Moore, G. R., and Williamson, D. J. (1988) *Biochem. J. 250*, 853−858.
45. Lloyd, E., Burk, D. L., Ferrer, J. C., Maurus, R., Doran, J., Carey, P. R., Brayer, G. D., and Mauk, A. G. (1996) *Biochemistry 35*, 11901−11912.
46. Bogumil, R., Hunter, C. L., Maurus, R., Tang, H.-L., Lee, H., Lloyd, E., Brayer, G. D., Smith, M., and Mauk, A. G. (1994) *Biochemistry 33*, 7600−7608.
47. Anni, H., and Yonetani, T. (1992) *Met. Ions Biol. Syst. 28*, 219−241.
48. Frew, J. E., and Jones, P. (1984) *Adv. Inorg. Bioinorg. Mech. 3*, 176−212.
49. Marquez, L. A., and Dunford, H. B. (1995) *J. Biol. Chem. 270*, 30434−30440.
50. Casella, L., Monzani, E., Gullotti, M., Santelli, E., Poli, S., and Beringhelli, T. (1996) *Gazz. Chim. Ital. 126*, 121−125.
51. Monzani, E., Gatti, A. L., Profumo, A., Casella, L., and Gullotti, M. (1997) *Biochemistry 36*, 1918−1926.
52. Davies, M. J. (1990) *Free Radical Res. Commun. 10*, 361−370.
53. Turner, J. J. O., Rice-Evans, C. A., Davies, M. J., and Newman, E. S. R. (1990) *Biochem. Soc. Trans. 18*, 1056−1059.
54. Onuoha, A. C., and Rusling, J. F. (1997) *J. Am. Chem. Soc. 119*, 3979−3986.
55. Dunford, H. B., and Stillman, J. S. (1976) *Coord. Chem. Rev. 19*, 187−251.
56. Segel, I. H. (1975) *Enzyme Kinetics*, Wiley, New York.
57. Hargrove, M. S., Wilkinson, A. J., and Olson, J. S. (1996) *Biochemistry 35*, 11300−11309.
58. La Mar, G. N., Toi, H., and Krishnamoorthi, R. (1984) *J. Am. Chem. Soc. 106*, 6395−6401.
59. Dunford, H. B. (1991) in *Peroxidases in Chemistry and Biology* (Everse, J., Everse, K. E., and Grisham, M. B., Eds.) Vol. II, pp 1−24, CRC Press, Boca Raton, FL.
60. Patterson, W. R., and Poulos, T. L. (1995) *Biochemistry 34*, 4331−4341.
61. Fukuyama, K., Kunishima, N., Amada, F., Kubota, T., and Matsubara, H. (1995) *J. Biol. Chem. 270*, 21884−21892.
62. Brantley, R. E., Smerdon, S. J., Wilkinson, A. J., Singleton, E. W., and Olson, J. S. (1993) *J. Biol. Chem. 268*, 6995−7010.
63. Ohlsson, P. J., Yonetani, T., and Wold, S. (1986) *Biochim. Biophys. Acta 874*, 160−166.

BI000784T